14th International Conference on Structural Safety and Reliability - ICOSSAR'25
1-6 June, 2025 - Los Angeles California, USA
R. Ghanem, E. Johnson, S. Masri and A. Olivier (Eds)

FRAGILITY ANALYSIS OF COASTAL BRIDGES DUE TO TSUNAMI-INDUCED WAVE LOADINGS

***Waqas Iqbal**[1], **Dr. Farahnaz Soleimani**[2]

[1] School of Civil & Construction Engineering, Oregon State University
Kearney Hall, 1491 SW Campus Way, Corvallis, OR 97331
iqbalw@oregonstate.edu, https://www.mainslab.net/

[2] School of Civil & Construction Engineering, Oregon State University
Kearney Hall, 1491 SW Campus Way, Corvallis, OR 97331
farahnaz.soleimani@oregonstate.edu, https://www.mainslab.net/

Key words: Tsunami Fragility Functions, Bridge Vulnerability Assessment, Finite Element Analysis, Tsunamis, Probabilistic Tsunami Demand Models (PTDMs), Bridge Fragility, Box Girder Bridges

Abstract. Recent seismic events in the Pacific Ocean have underscored the immense destructive potential of tsunamis, highlighting the need for robust engineering strategies to protect critical infrastructure. Existing research on tsunami-induced fragility functions predominantly focuses on quasi-static pressure distributions over infrastructure components, which often oversimplify the complex and dynamic nature of tsunami wave forces. This study bridges this gap by conducting a time history analysis of box girder bridges under dynamic wave loadings to develop fragility functions more reflective of real-world conditions. Leveraging linear wave theory, wave particle acceleration time histories are derived from tsunami inundation depths, which are stochastically generated through Latin Hypercube Sampling to ensure comprehensive coverage of potential scenarios. These acceleration profiles serve as input for finite element analysis of box girder bridges, enabling the evaluation of column ductility demand as the engineering demand parameter (EDP). The finite element analysis accounts for both material and geometric nonlinearities to capture the complex response of bridge structures under transient dynamic loads. The results inform the development of probabilistic tsunami demand models (PTDMs) via regression, which correlate EDPs with wave intensity measures such as peak wave acceleration. Fragility functions are then derived for various damage levels, capturing the progressive failure mechanisms of bridge components and system under varying levels of dynamic wave loading. These functions provide critical insights into the likelihood of structural failure at different tsunami intensities, offering a more nuanced understanding of bridge vulnerabilities. This research establishes a dynamic-focused framework for assessing and predicting bridge failures in tsunami-prone regions.

* *Corresponding Author*

1 Introduction

Bridges are essential for maintaining connectivity during and after natural disasters such as earthquakes and tsunamis. Seismic and tsunami hazards are significant threats to bridge structures, particularly in coastal and seismically active regions. The performance of these structures during such events is influenced by various factors, including bridge design, material properties, site conditions, and the characteristics of the seismic or tsunami event itself. The seismic performance of bridges is a key concern for infrastructure resilience in seismically active regions. Extensive studies have investigated the impact of earthquake-induced forces on bridge behavior, with particular attention given to factors such as ground shaking, fault displacement, and structural response. Studies such as those by [1], and [2] have examined the vulnerability of bridge structures to seismic events. These studies highlight the importance of identifying critical structural components, such as columns, abutments, and foundations, that experience significant damage during an earthquake. As a continuation of this study, [3] examined the influence of bridge irregularities on structural damage, functionality loss, increased repair costs, and safety risks. Recent advancements in seismic design methods have focused on improving the resilience of bridge structures to both ground shaking and fault movements. The use of advanced materials such as fiber-reinforced polymers (FRP) and the implementation of innovative design strategies, such as base isolation and energy dissipation devices, have been proposed to enhance the seismic performance of bridges [4]. Numerical simulations and experimental tests have also been employed to evaluate the seismic response of bridge structures which provide valuable insights into the deformation mechanisms and failure modes of bridges during earthquakes. Additionally, there have also been recent extensive studies in the determination of the performance of bridges using machine learning (ML) techniques such as ML models for probabilistic seismic demand models [5], the efficiency of a variety of parametric and non-parametric ML algorithms with different degrees of flexibility to estimate the demands associated with the primary bridge components [6], and a kernel-based Gaussian regression approach, to estimate the column drift ratio metric for bridges [7]. Other studies conducted by [8] and [9] also presented the first ensemble learning-based predictive model using bagging and boosting techniques to predict resilience index as a function of seismic events and asset characteristics on bridge resilience. While seismic performance has been extensively studied, the unique and complex challenges posed by tsunami loading on bridge structures have only more recently gained focused attention.

Tsunamis present a distinct set of challenges for bridge performance, with the potential for large wave forces, scour, and debris impact to cause significant damage to bridge foundations and superstructures. There have been extensive damages to reinforced concrete pre-stressed bridges due to the washing away of girders and also the splitting of bridge piers near the bottom of the pier due to larger base shears generated by larger wave pressures resulting from large impact durations. As well as there were also damage to side stoppers used for resisting lateral movements as tsunami waves not only imparted horizontal forces but also buoyant forces that resulted in the uplift forces that are not present in the case of seismic events. These cases have been highlighted in one of the case studies conducted by [10] after the 2011 Tohoku tsunami in Japan. Research by [11] and [12] has also investigated the impact of tsunami waves on bridge structures. The forces exerted by tsunami waves on bridges are highly variable and depend on factors such as wave height, wave period, and the configuration of the bridge. Additionally, tsunami-induced scour is a major concern for bridge foundations located in coastal areas. Studies such as those by [13] and [14] have explored the effects of tsunami-induced

scour on bridge foundation stability. The interaction between tsunami waves and the soil around bridge foundations can lead to significant erosion, undermining the structural integrity of the bridge. Dynamic and complex nature of wave particle motion emphasize the need of extensive research on wave structure interaction studies to derive empirical relationships to get equivalent static forces imparted by wave motion. One of the studies conducted by [15] performed an experimental study on a bridge prototype in large wave flume at the O.H. Hinsdale Wave Research Laboratory at Oregon State University in which wave pressures, and forces acting on specimen were recorded to develop force versus wave height correlation. Additionally, for the specific prototype, dynamic response was also recorded in terms of vertical force time history. In another study conducted by [16], fragilities for probabilistic tsunami damage assessment were developed based on FEMA models. Another study conducted by [17] used dynamic wave time histories to study the shear response of bearing pads in case of hurricanes, but there were no other components and system-level damages included in that study. Although there have been many more studies conducted in the past using wave time histories for structural response, but there is still need of including dynamic nature of wave forces on different bridge components as according to authors knowledge there has not been such study conducted where dynamic response of bridges due to tsunami dynamic wave time histories has been conducted with varying bridge configurations and intensity measure as wave acceleration. This research study is focused on the non-linear dynamic response of set of box girder bridge samples using dynamic wave time histories hence taking the real-time dynamic response of structure instead of static response that could under or overestimate the responses.

2 Methodology

2.1 Tsunami-Induced Wave Loadings

This study uses linear wave theory and Latin Hypercube Sampling (LHS) to generate representative tsunami wave acceleration time histories. LHS is a statistical method used for generating a sample of plausible inputs from a multidimensional distribution [18]. The equation defining LHS, Eq. 1 , ensures that each variable is sampled uniformly across its range, avoiding clustering.

$$X_i = F^{-1}\left(\frac{P_i + U_i}{N}\right), \quad i = 1, 2, ..., N \tag{1}$$

In Eq. 1, X_i is the sampled value of the variable,F^{-1} is the inverse cumulative distribution function (CDF) of the variable, P_i is a permutation of indices $(0, 1, \ldots, N-1)$, $U_i \sim U(0, 1)$ is a uniformly distributed random number in $[0, 1]$, and N is the total number of samples. For lower and upper limits of sampling, wave heights, and wave period distribution functions are taken from [19] in which wave heights were recorded by tidal gauges throughout the Pacific Ocean for 2015 Chile earthquake. Using LHS as mentioned in Eq. 1, 160 random sample combinations are produced as shown in Figure 1(a). The spread of points in the plot captures a broad spectrum of wave conditions, from small, frequent waves to large, infrequent storm waves. LHS ensures a well-distributed and representative set of wave conditions, avoiding clustering and gaps in data. Due to real-world wave conditions highly variability, capturing a wide range ensures more accurate structural response predictions.

Airy's theory [20] is used in this study to calculate wave time history acceleration using the velocity potential, $\phi(x, z, t)$, as stated in Eq. 2, and then differentiating velocity potential to compute wave

horizontal acceleration as stated in Eq. 3. These are then used to generate 320 wave time histories with 160 in both longitudinal and transverse direction.

$$\phi(x,z,t) = \frac{a \cdot g}{\sigma} \cdot \frac{\cosh k(d+z)}{\cosh(kd)} \cdot \sin(kx - \sigma t) \tag{2}$$

$$ax = \frac{\partial \phi}{\partial x} = \frac{2\pi^2 H}{T^2} \cdot \left[\frac{\cosh k(d+z)}{\sinh(kd)}\right] \cdot \sinh(kx - \sigma t) \tag{3}$$

Where; a represents wave amplitude, g is gravitational acceleration, σ represents wave angular frequency, k is wave number, d is still water depth, z is vertical elevation from still water depth, and x is horizontal coordinate along the wave direction. The first three generated wave time histories are shown in Figure 1(b). It has been observed that wave accelerations range from 0 to 40 in/sec² which is in the range of accelerations for intermediate to shallow waters determined based on the computation of tsunami eigenfunctions using Airy's theory and dispersion relationships [21]. This can also be supported by the collapse of the Tsutanigawa railway bridge in the 2011 Tohoku Tsunami which was approximately 1.6 km away from the coastline hence emphasizing larger wave forces resulting in larger column deflections as provided in detail by [10].

2.2 Finite Element Modeling

As a case study, a two-span box girder bridge with a rigid diaphragm abutment with characteristics of the pre-1970 design era was selected for which the OpenSees [22] model is shown in Figure 1(c). The fiber section model is used for column elements using concrete cover and core material as Concrete07, and steel material as Steel02. This fiber section model is used to induce material nonlinearity for bridge columns. The bridge deck and transverse rigid diaphragms are modeled as elastic beamcolumn elements. Abutments are modeled as zerolength spring elements with hyperbolicGap material for active and passive displacements of abutments in the longitudinal direction of the bridge. However, abutment piles are modeled as linear spring elements using hysteretic uniaxial material for determination of piles longitudinal translation. Bent columns foundation is modeled as linear and rotational springs with elastic uniaxial material. More modeling details can be found in [23].

2.3 Non-linear Dynamic Response History Analysis

Non-linear dynamic response history analysis (NLRHA) is used to predict the bridge components and bridge system response due to wave loadings. Wave loadings are applied both along the longitudinal and transverse in-plane axis. Directionality is being taken care of by bridge modeling parameters for producing 160 random box girder bridge samples. A total of 160 box girder bridge samples are generated based on geometric data like girder spacing, deck width, column height, etc., and material properties like soil stiffness, and concrete and steel strength. Response histories are recorded for deck displacements, column curvature, abutment active and passive translation, foundation translation and rotation, and abutment transverse displacements. For all components other than the deck slab, element envelope responses are captured from their respective time histories. However, the displacement response of the deck for 12 different nodes along the bridge longitudinal axis is recorded and shown in Figures 2(a) and 2(b). Deck displacement response shows maximum displacement of around 0.12 inches which is in close agreement with some other studies like the one conducted by [24], in which transverse deck displacement of 0.2 inches was recorded. However, the difference in

displacement can be attributed to different bridge type as three-span reinforced-concrete (RC) I-girder bridge superstructure.

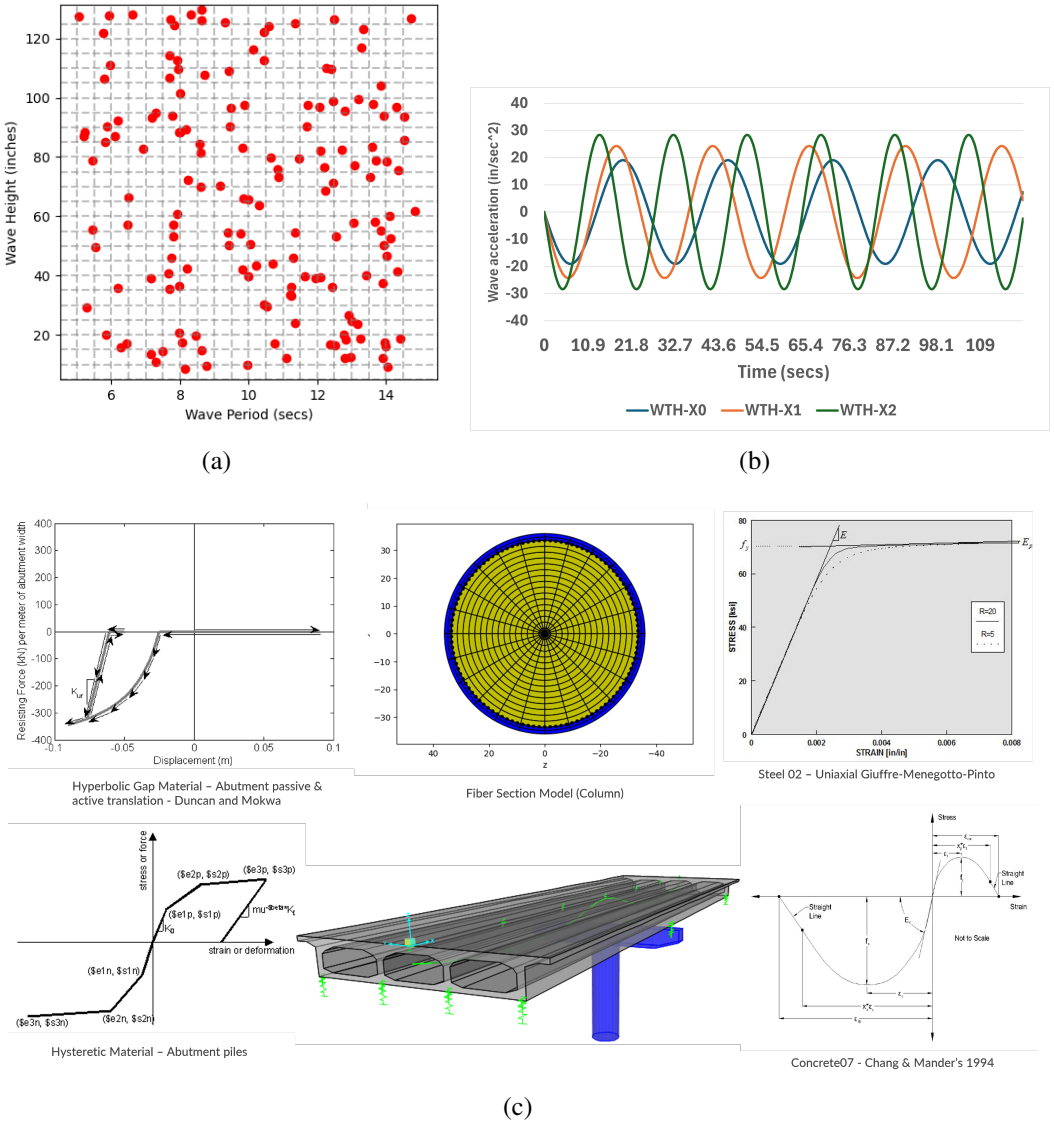

(a) (b)

(c)

Figure 1: (a) Latin Hypercube Sampling, (b) Wave Time histories, (c) Bridge Finite Element Model

2.4 Fragility Functions

Bridge damage due to natural hazard events like Tsunamis events is commonly represented by a damage probability matrix or fragility function for describing the performance of bridges under engineering demand. A fragility function is a conditional probability statement that provides the likelihood of a structure to withstand specified levels of damage for a given intensity measure as given in Eq. 4. These functions provide a probabilistic assessment of structure at different levels of input intensity, unlike deterministic performance design criteria as safe or unsafe. Eq. 4 expresses the fragility function in terms of demand D and capacity C, where S_D and S_C represent the median values of demand and capacity, respectively. The parameters $\beta_{D|IM}$ and β_C denote the dispersions (logarithmic standard deviations) of the demand and capacity, respectively.

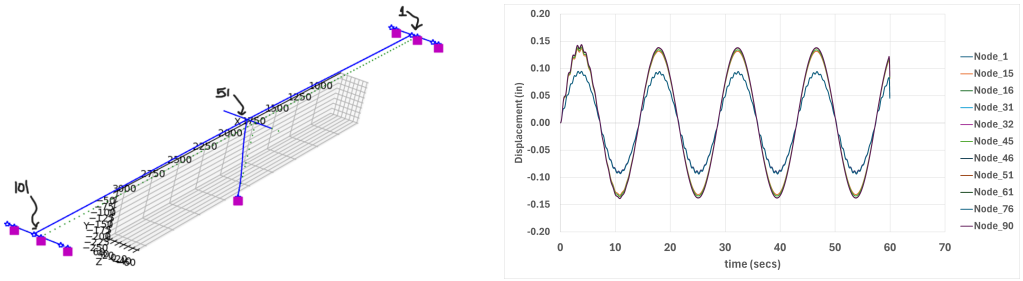

(a) (b)

Figure 2: (a) Deformed Shape @ 55 secs, (b) Deck displacement time histories (in)

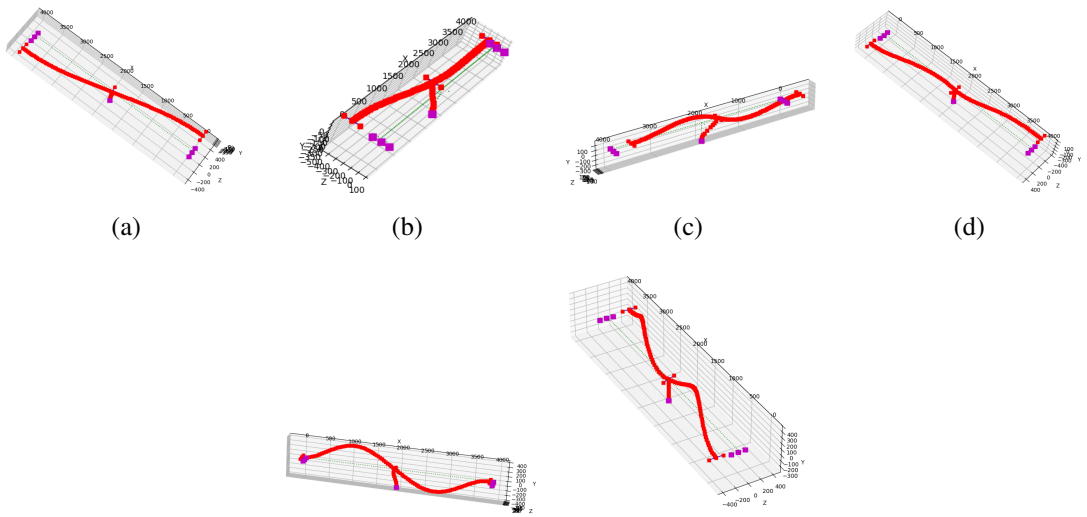

(a) (b) (c) (d)

(e) (f)

Figure 3: Mode shapes # (a) 1, (b) 2, (c) 3, (d) 4, (e) 5, (f) 6

These dispersions account for the uncertainty in how demand and capacity are distributed around their respective median values. Importantly, the capacity S_C and its associated dispersion β_C are defined based on the specific limit state being considered, as each limit state represents a different level of damage or failure for the bridge. Estimates of system reliability, particularly when considering the vulnerability of multiple components in a structure, can be obtained by combining the individual Probabilistic Tsunami Demand Models (PTDMs) of each component to create a Joint Probabilistic Tsunami Demand Model (JPTDM). This approach involves convolving the PTDMs, which represent the probabilistic relationship between tsunami demand and the response of individual components, to develop a more comprehensive model that captures the behavior of the entire system. Once the JPTDM is established, the next step is to integrate it over all possible failure domains (or limit states) to compute the probability of the system exceeding a particular damage level at a specific Intensity Measure (IM).

$$P[D > C \mid IM] = \Phi\left(\frac{\ln(S_D/S_C)}{\sqrt{\beta^2_{D|IM} + \beta^2_C}}\right) \tag{4}$$

Engineering demand parameters (EDPs) and their component damage thresholds are mentioned in Table 1. For columns, components damage thresholds (CDTs) are based on [25] in which CDT-0 represents cracking, CDT-1 represents minor cover concrete spalling anywhere along the column, CDT-2 represents large shear cracks; major spalling; exposed core; confinement yield (No rupture), and CDT-3 represents a loss of confinement; longitudinal bar buckling; and core crushing. However, the column's post-yield behavior is more ductile which is defined by increased EDPs compared to pre-1971 era bridges. For superstructure deck, CDTs are based on the Caltrans design engineers [26] which are based on observed displacements during past earthquakes and this provides a critical trigger for a thorough inspection of bridges for any damages globally or locally. In general, abutment back walls are designed to shear off in which passive response is based on the deflection at the top of the back wall while active and transverse responses are dependent upon yielding and ultimate deformation of piles. For foundation CDTs, foundation translation is consistent with the abutments translation however foundation rotation is the cause of axial pile movement at the one edge of the pile cap hence producing the overturning moment. Bridge system level thresholds (BSSTs) are classified into four categories; BSST-0 (Minor Damage), BSST-1 (Moderate Damage), BSST-2 (Extensive Damage), and BSST-3 (Complete Damage). These system-level damage states are dependent on the component level damage thresholds like BSST-0 refers to CDT-0 (No damage) to CDT-1 (Aesthetic damage), BSST-1 refers to CDT-1 (Aesthetic damage) to CDT-2 (Repairable minor functional damage), BSST-2 refers to CDT-2 (Repairable minor functional damage) to CDT-3 (Repairable major functional damage), and BSST-3 refers to component replacement [23].

Table 1: Median (Med) and Dispersion (Disp) values for different components across CDT levels [23].

Component	**Symbol**	**CDT-0**		**CDT-1**		**CDT-2**		**CDT-3**	
		Med	**Disp**	**Med**	**Disp**	**Med**	**Disp**	**Med**	**Disp**
Columns - Curvature Ductility	μ_ϕ	0.80	0.35	0.90	0.35	1.00	0.35	1.20	0.35
Maximum deck displacement (in)	δ_{deck}	0.16	0.35	0.48	0.35	4.00	0.35	6.00	0.35
Foundation translation (in)	δ_{fnd}	0.04	0.35	0.16	0.35	6.00	0.35	6.00	0.35
Foundation rotation (rad)	θ_{fnd}	0.015	0.35	0.06	0.35	1.00	0.35	1.50	0.35
Passive abutment displacement (in)	δ_a	0.12	0.35	0.40	0.35	4.00	0.35	6.00	0.35
Active abutment displacement (in)	δ_p	0.06	0.35	0.16	0.35	4.00	0.35	6.00	0.35
Transverse abutment displacement (in)	δ_t	0.04	0.35	0.16	0.35	4.00	0.35	6.00	0.35

3 Results

Figure 3 presents the first six mode shapes of the bridge, which provide critical insights into its dynamic behavior as modal contribution of first 6 modes is used to get bridge component responses. The first mode shape in Figure 3(a) primarily exhibits longitudinal bending, with maximum deformation occurring at mid-span while the supports remain relatively stationary. This fundamental mode is crucial in assessing the bridge's vulnerability to wave-induced resonance and overall structural stability. The second mode shape in Figure 3(b) introduces torsional deformation, where the bridge deck twists along its longitudinal axis. This type of response is significant when considering asymmetric wave

loads, differential ground motion during earthquakes, or oblique hydrodynamic forces. As the modes progress, the third and fourth mode shapes in Figure 3(c) and 3(d) reveal higher-order bending deformations, characterized by multiple inflection points along the span. These modes indicate localized stress concentrations and fatigue-prone regions, which are particularly important when evaluating the cumulative effects of repeated wave impacts and vortex-induced vibrations. The fifth mode shape in Figure 3(e) is primarily associated with lateral bending, where the deck moves sideways rather than vertically. This response is a crucial factor when assessing hydrodynamic loading from waves, lateral drift due to strong currents, or seismic-induced lateral forces. Finally, the sixth mode shape in Figure 3(f) represents a complex combination of torsion and lateral bending, where both twisting and sideways displacements occur simultaneously.

Response time histories using NLRHA and intensity measures as peak wave acceleration are used to determine PTDMs for each bridge component. From PTDMs shown in Figure 4, it can be observed that there is a strong correlation between intensity measure (IM) and demand parameters for all bridge components. Regression coefficients from these regression plots are then used to calculate the cumulative probability of damage to each component given the intensity measure as peak wave acceleration. The fragility curves presented in Figure 5(a) illustrate the probability of exceeding CDT-0 as a function of wave acceleration (WA) for various bridge components, including columns, deck slabs, foundations, and abutments. The curve for columns (solid blue line) shows a steep increase in probability at relatively low WA values, indicating that concrete cracking to columns occurs at even modest wave forces induced by wave acceleration of 10 in/sec². This suggests that columns are highly susceptible to minor surface damage under wave loading.

Other structural components exhibit more gradual fragility trends. The deck slab (yellow dashed line) starts exceeding the displacement thresholds around 7 in/sec², with approaching failure at approximately 10 in/sec² emphasizing the need for inspection even at lower damage state levels. The foundation rotation is represented by a purple line having the lowest fragility with little lag till the peak wave acceleration reaches 15 in/sec². This could be due to the reason that piles are not having substantial differential axial deformations. However, the foundation translation indicated by the orange line has a higher probability of exceedance starting at 6 in/sec² and approaching failure at 15 in/sec². The abutment active translation shown by a magenta color dashed line shows almost the same behavior indicating that the same amount of foundation and abutment active translation i.e. abutment's movement towards the soil. The abutment's passive translation represented by a green dashed line starts at around 7 in/sec² with almost approaching failure at 25 in/sec² showing the piles lateral resistance in the bridge longitudinal direction hence avoiding the abutment's passive movement. Abutment transverse displacement is directly dependent on piles lateral movement in the direction perpendicular to the bridge axis which can be further validated by the fact that deck displacements exceed the limit after the abutment transverse displacement due to both piles lateral displacements and superstructure transverse movement as well.

The fragility curves presented in Figure 5(b) present the same pattern but with lag in exceeding the limit state with columns being still more vulnerable and with the difference that for CDT-1, abutment passive translation is less vulnerable compared to foundation rotation for CDT-0. Similarly, in Figure 5(c) and Figure 5(d), it can be observed that abutment transverse displacement starts exceeding limits beyond 13 in/sec² and 15 in/sec² for CDT-2 and CDT-3, respectively. While all other components showed maximum resistance even till the wave acceleration of 40 in/sec². This overall indicates

that for higher level damage states, columns are most vulnerable and abutments are the second most vulnerable in their transverse displacement due to both piles and superstructure imparted motions. Bridge system fragility curves shown in Figure 5(e) indicate that the overall bridge system starts responding at around 1.8 in/sec² with very quickly increasing vulnerability by 4 in/sec² and this is due to the most influenced response of columns within range of 5 in/sec².

4 Conclusions & Recommendations

This research presents a rigorous seismic and hydrodynamic vulnerability assessment of a coastal bridge using nonlinear time history analysis. By integrating wave acceleration time histories derived from Airy's wave theory, the study captures the complex response of coastal box girder bridges under these extreme forces. The fragility analysis highlights that bridge columns are the most vulnerable structural components, whereas abutment piles with higher lateral movements and less axial differential movement. This could be refined more as for this study foundation translational and rotational stiffness are based on the soil data from bore logs at the bridge locations using shear wave velocity and angle of friction. However, there is a great potential for detailed soil structure interaction for exactly predicting the response. Additionally, simple linear wave theory is used for this study however that does not stay valid for higher wave heights as near shore due to the geological structure of earth wave height increases while particle velocity and acceleration approach zero. So, for larger tsunami wave heights, it would be crucial to test appropriate wave theories such as non-linear wave models like Stokes 5th order or Conoidal theory to make a comparison.

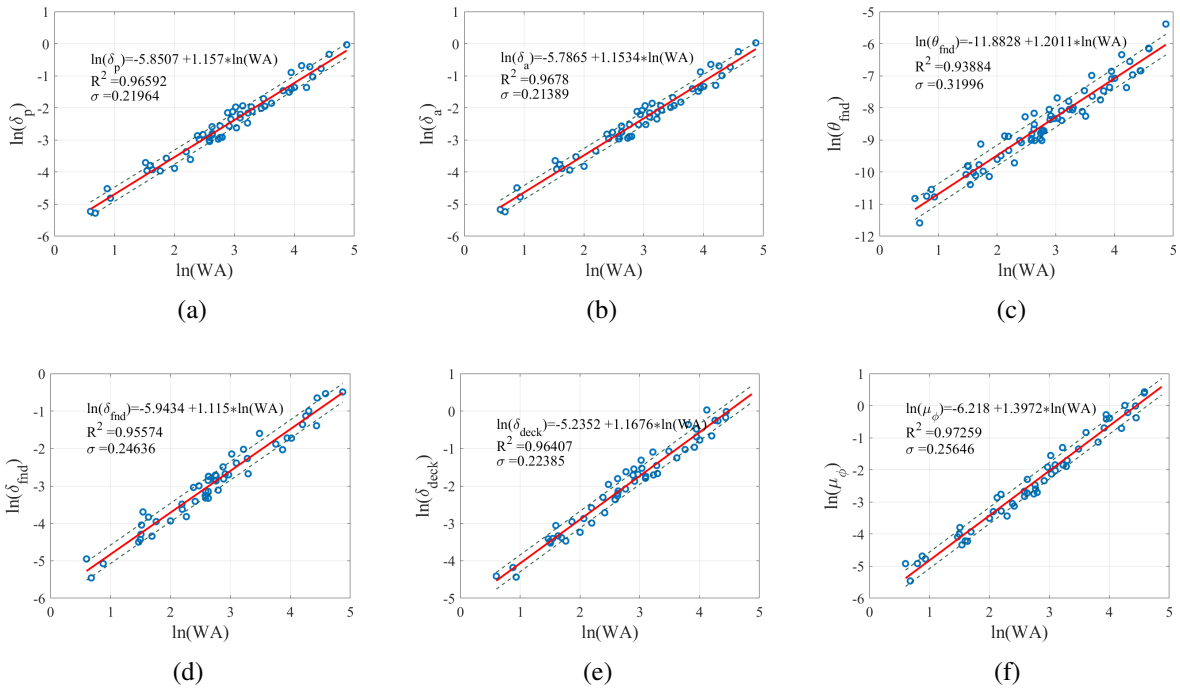

Figure 4: PTDMs for: (a) Abutment passive translation (in), (b) Abutment active translation (in), (c) Foundation rotation (rads), (d) Foundation translation (in), (e) Deck displacement (in), (f) Column Curvature

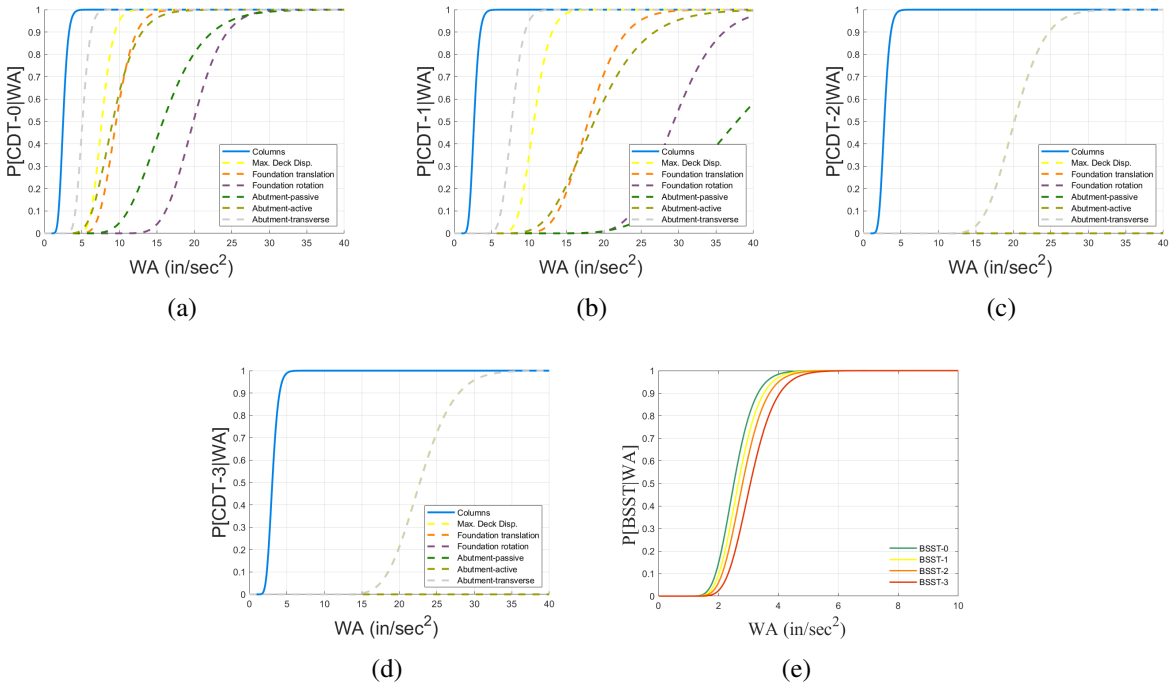

Figure 5: Fragility Curves for: (a) CDT-0, (b) CDT-1, (c) CDT-2, (d) CDT-3, (e) BSST - Bridge system level thresholds

5 Data Availability Statement

Data can be reproduced by the corresponding author on demand.

References

[1] J. Wang and Y. Zhang. "Seismic vulnerability assessment of bridge structures". In: *Journal of Earthquake Engineering* 20.2 (2016), pp. 335–357.

[2] Farahnaz Soleimani, Sujith Mangalathu, and Reginald DesRoches. "A comparative analytical study on the fragility assessment of box-girder bridges with various column shapes". In: *Engineering Structures* 153 (2017), pp. 460–478.

[3] Farahnaz Soleimani et al. "Identification of the significant uncertain parameters in the seismic response of irregular bridges". In: *Engineering Structures* 141 (2017), pp. 356–372.

[4] S. Li and X. Zhang. "Seismic design of bridges with fiber-reinforced polymers". In: *Structural Engineering and Mechanics* 71.4 (2019), pp. 455–472.

[5] Farahnaz Soleimani and Donya Hajializadeh. "State-of-the-art review on probabilistic seismic demand models of bridges: Machine-learning application". In: *Infrastructures* 7.5 (2022), p. 64.

[6] Farahnaz Soleimani. "Probabilistic seismic analysis of bridges through machine learning approaches". In: *Structures*. Vol. 38. Elsevier. 2022, pp. 157–167.

[7] Sonia Zehsaz, Sabarethinam Kameshwar, and Farahnaz Soleimani. "Kernel-based Column Drift Ratios Prediction in Highway Bridges". In: (2024).

[8] Farahnaz Soleimani and Donya Hajializadeh. "Bridge seismic hazard resilience assessment with ensemble machine learning". In: *Structures*. Vol. 38. Elsevier. 2022, pp. 719–732.

[9] F Soleimani and D Hajializadeh. "Analytical seismic resilience identifiers of bridges". In: *Bridge Maintenance, Safety, Management, Digitalization and Sustainability*. CRC Press, 2024, pp. 1583–1591.
[10] Mitsuyoshi Akiyama et al. "Reliability of bridges under tsunami hazards: Emphasis on the 2011 Tohoku-oki earthquake". In: *Earthquake Spectra* 29.1_suppl (2013), pp. 295–314.
[11] S. Yan and Y. Chen. "Tsunami loading on bridge structures: A review". In: *Coastal Engineering* 123 (2017), pp. 52–63.
[12] Z. Xu and X. Li. "Impact of tsunami waves on the seismic performance of coastal bridges". In: *Journal of Tsunami Research* 12.3 (2019), pp. 213–229.
[13] D. Smith and L. Wang. "Tsunami scour effects on bridge foundations: Numerical modeling and analysis". In: *Geotechnical Engineering* 40.2 (2020), pp. 150–168.
[14] R. Mishra and V. Patel. "Modeling tsunami-induced scour around bridge piles". In: *Coastal Engineering Journal* 63.4 (2021), pp. 398–410.
[15] Christopher Bradner et al. "Experimental setup for a large-scale bridge superstructure model subjected to waves". In: *Journal of waterway, port, coastal, and ocean engineering* 137.1 (2011), pp. 3–11.
[16] Hyoungsu Park, Daniel T Cox, and Andre R Barbosa. "Comparison of inundation depth and momentum flux based fragilities for probabilistic tsunami damage assessment and uncertainty analysis". In: *Coastal Engineering* 122 (2017), pp. 10–26.
[17] Waqas Iqbal and Monique Head. "Parametric study for shear failure of bearing pads due to hurricane-induced wave loadings". In: *Advances in Bridge Engineering* 5.1 (2024), p. 30.
[18] M. D. McKay, R. J. Beckman, and W. J. Conover. "A Comparison of Three Methods for Selecting Values of Input Variables in the Analysis of Output from a Computer Code". In: *Technometrics* 21.2 (1979), pp. 239–245. DOI: 10.1080/00401706.1979.10489755.
[19] Paula Dunbar et al. "Challenges in defining tsunami wave heights". In: *Pure and Applied Geophysics* 174 (2017), pp. 3043–3063.
[20] George B Airy. "Tides and waves. encyclopaedia metropolitana (1817–1845)". In: *Mixed Sciences, edited by HJ Rose* 3 (1841), p. 1841.
[21] Sudhir Kumar Chaturvedi, Ugur Guven, and Pankaj Kumar Srivastava. "Measurement and validation of tsunami Eigen values for the various water wave conditions". In: *Journal of Ocean Engineering and Science* 5.1 (2020), pp. 41–54.
[22] Frank McKenna. "OpenSees: a framework for earthquake engineering simulation". In: *Computing in Science & Engineering* 13.4 (2011), pp. 58–66.
[23] Farahnaz Soleimani. "Fragility of California bridges-development of modification factors". In: *Doctoral diss., Georgia Institute of Technology* (2017).
[24] Jesika Rahman and AHM Muntasir Billah. "Development of performance-based fragility curves of coastal bridges subjected to extreme wave-induced loads". In: *Journal of Bridge Engineering* 28.3 (2023), p. 04023005.
[25] Marc J Veletzos et al. *Visual inspection & capacity assessment of earthquake damaged reinforced concrete bridge elements*. Tech. rep. 2008.
[26] Highway Design Manual. "Caltrans". In: *Sacramento, California, USA* (2014).